*Journal of Applied Electrochemistry* **32**: 735–741, 2002.



# Ir-based oxide electrodes: oxygen evolution reaction from mixed solvents

A. ROSSI[1] and J.F.C. BOODTS[1,2,*]
[1]*Chemistry Department, FFCLRP, University of São Paulo, Av. Bandeirantes 3900, 14040-901, Ribeirão Preto, SP, Brazil*
[2]*Chemistry Institute, Federal University of Uberlândia, Av. João Naves de Ávila 2160, 38400-902, Uberlândia, MG, Brazil*
*(*author for correspondence, fax: +55 16 633 8151, e-mail: jfcboodts@ufu.br)*

Received 9 April 2001; accepted in revised form 16 April 2002

*Key words:* cosolvent influence, electrode kinetics, iridium dioxide, oxygen evolution reaction

**Abstract**

The influence of 30% (v/v) organic cosolvent in 1.0 mol $dm^{-3}$ $HClO_4$ on the OER electrode kinetics, surface properties and electrode stability of $IrO_2$-based electrodes was investigated by cyclic voltammetry and polarization curves. The Tafel coefficients in the presence of cosolvent are explained in terms of the change of the rate-determining step (r.d.s.) of the OER electrode mechanism, coating dissolution and/or cosolvent oxidation. Of the several cosolvents investigated *t*-BuOH and PC show less effects on the OER and electrode properties making them the best choice for organic eletrosynthesis applications, in contrast to AN, which causes coating dissolution, and DMF and DMSO which show an anticipation of the voltammetric current.

## 1. Introduction

The nature of the electrode material strongly affects the efficiency for the OER [1]. Among the several electrode materials available, one of the most efficient for the OER are Ti-supported $IrO_2$-based dimensionally stable anodes, DSA® [2, 3]. The excellent electrocatalytic and mechanical properties of this catalyst ($IrO_2$) has stimulated its application in electrochemical oxidation of organic substrates, normally combined with the OER [4, 5]. An important advantage of this kind of electrode material, besides their good electrocatalytic and mechanical properties, is that the catalyst is immobilized thus facilitating its recovery from the reaction mixture, and reducing the number of steps necessary to isolate the products.

Despite the several desirable properties, application of $IrO_2$-based (and similar) electrode materials to organic electrosynthesis is still underexploited [6]. One of the main problems is the blocking of the electrode surface frequently observed with organic substrates, particularly with aromatic substrates. Recently, it was shown that the oxidation of organics when carried out simultaneously with the OER significantly reduces the surface blocking process [7]. One of the authors showed [8] that blocking of $Ti/RuO_2$ and $Ti/IrO_2$ surfaces is mainly due to surface film formation as a consequence of organic radical dimerization/polymerization. Oxidation done in the OER region can not only recover already spoiled surfaces but also avoids blocking of the electrode surface. This was attributed to the mechanical action of intense $O_2$ evolution, which favours the removal and/or avoids fixation of the organic film, combined with film oxidation by the several radical species involved in the OER electrode process [5].

Because of the limited solubility of numerous organics in water, the use of an organic cosolvent is a frequently encountered experimental situation in organic electrochemistry. Only a limited number of papers deal with the investigation of the influence of organic solvents on the OER [7, 9]. Zanta et al. [7] investigated the surface and catalytic properties of $Ti/RuO_2$ and $Ti/IrO_2$ electrodes in non-aqueous media showing these properties are significantly affected by both the cation of the supporting electrolyte and the chemical nature of the solvent. These authors also observed an anodic displacement of up to 300 mV (e.g., acetonitrile (AN) and propylene carbonate (PC)) of the OER.

In this paper we report the influence of mixed solvents on the surface properties and the OER of $TiO_2$ stabilized $IrO_2$-based electrodes.

## 2. Experimental details

### 2.1. *Electrodes*

Oxide layers of nominal composition $Ir_xTi_{(1-x)}O_2$ ($x = 0.3$, 0.7 and 1.0) were deposited on both sides of sand-blasted Ti supports (10 mm × 10 mm × 0.2 mm),

previously etched for 20 min in boiling oxalic acid (10% w/w), by thermal decomposition ($T_{calc}$: 400 °C; $t_{calc}$: 1 h; $O_2$ flux: 5 L $min^{-1}$) of the adequate precursor mixture prepared from 0.10 mol $dm^{-3}$ precursor solutions of $IrCl_3 \cdot nH_2O$ (Aldrich) and $TiCl_4$ (Ventron) dissolved in 1:1 (v/v) HCl (Merck). The precursor mixture was spread on both faces of the Ti-support by brush. The residue obtained after solvent evaporation at about 80 °C was calcined for 10 min in a preheated furnace. The operation was repeated (three or four applications were necessary) until the desired oxide loading was reached (a nominal layer thickness of about 2 $\mu$m requires, depending on composition, between 1.3 and 2.3 mg $cm^{-2}$ of oxide loading). A final firing for 1 h, using the same experimental conditions, completed the procedure.

### 2.2. *Solutions*

All studies were carried out using aqueous 1.0 mol $dm^{-3}$ $HClO_4$, containing 30% (v/v) of cosolvent, as supporting electrolyte. The water used was of Milli-Q quality (Millipor; $R \geqslant 18.2$ MΩ). Cosolvents investigated were: acetonitrile, AN (Mallinckrodt, HPLC); *t*-butanol, *t*-BuOH, (Mallinckrodt, AR); *N*,*N*-dimethylformamide, DMF (Merck, Uvasol); dimethylsulfoxide, DMSO (Merck, Uvasol), and propylene carbonate, PC (Aldrich, 99%). All chemicals were used as received without further purification. Solutions were deaerated by nitrogen bubbling before and during experiments. The study was carried out at room temperature (25 ± 0.5 °C).

### 2.3. *Electrochemical measurements and instrumentation*

Experiments were carried out in an air-sealed conventional glass cell having separate compartments for: (i) the working and the reference electrodes (Ag/AgCl, 0.1 mol $dm^{-3}$ NaCl, separated from the solution by a Luggin capillary); (ii) two coiled heavily platinized platinum wires, used as counter electrodes, placed symmetrically at both sides of the working electrode. Medium-pore glass discs separated the working and counter electrode compartments. Experimental data were recorded using an EG&G model 273A potentiostat/galvanostat. Tafel curves were recorded under quasi-stationary conditions (0.056 mV $s^{-1}$) initially moving the potential anodically until a current of about 100 mA was observed (anodic sweep). Next, without interruption of the procedure, the potential sweep was inverted (cathodic sweep) until the initial potential was reached again. The anodic/cathodic potential sweep sequence was executed twice, without interruption.

### 2.4. *Electrode preconditioning*

To avoid possible surface blocking and improve reproducibility of the results, the electrode was submitted, before each voltammetric experiment, to a pretreatment which consisted in the application for 90 min of a constant anodic current of 100 mA. The pretreatment was carried out in a separate aqueous 1.0 mol $dm^{-3}$ $HClO_4$ and is of particular importance in the case of freshly prepared coatings which, under intense oxygen evolution, frequently show a significant increase in electrochemically active surface area, before a state of equilibrium is reached. This activation of the electrode under conditions of intense oxygen evolution is attributed to the hydration of surface sites localized in difficult-to-reach oxide regions (pores, small cracks etc.) [10]. Since currents of the same magnitude are reached during the recording of Tafel curves, the pretreatment procedure must be applied to avoid changes in the electrochemically active surface area of the electrode while the Tafel curves are recorded.

## 3. Results and discussion

### 3.1. *Cyclic voltammetry*

Cyclic voltammograms, CV, representative of the behaviour of the electrode materials in 1.0 mol $dm^{-3}$ $HClO_4$, in the absence and presence of 30% (v/v) cosolvent, are shown in Figure 1.

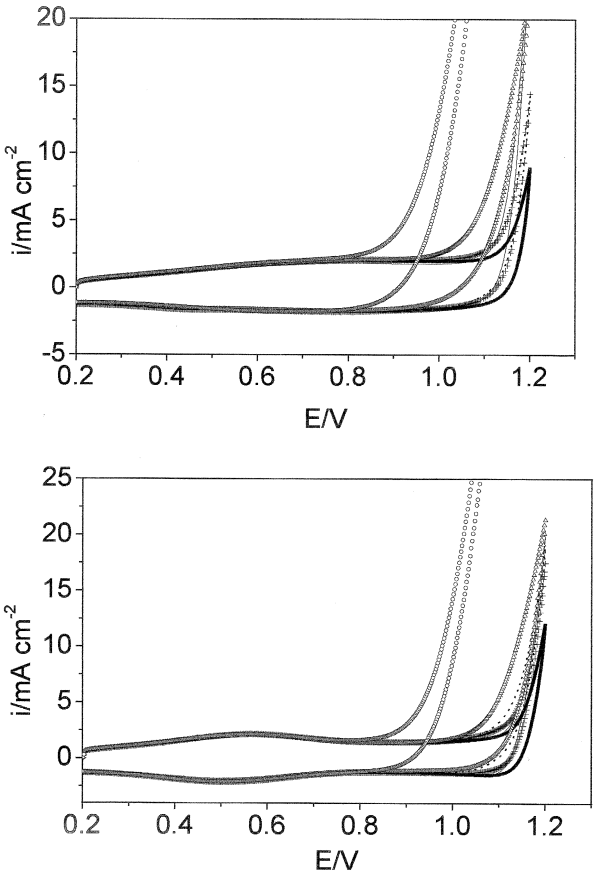


*Fig. 1.* Cyclic voltammograms of (a) $Ti/IrO_2$ and (b) $Ti/Ir_{0.3}Ti_{0.7}O_2$ electrodes from 1.0 mol $dm^{-3}$ $HClO_4$ (—) and in the presence of 30% (v/v) cosolvent: (▬) AN; (+) *t*-BuOH; (- - -) PC; (Δ) DMF; (○) DMSO. $v = 20$ mV $s^{-1}$.

In the absence of the cosolvent the CV shows a large band, localised in the 0.4–0.8 potential region, attributable to the Ir(III)/Ir(IV) solid state surface redox transitions, SSSRT. The band is best defined with the Ti/$Ir_{0.3}Ti_{0.7}O_2$ nominal composition. OER starts around 1.1 V. This behaviour is in agreement with the literature [11].

The introduction of 30% (v/v) of cosolvent to the supporting electrolyte does not affect the localization of the SSSRT or the SSSRT current. These results show that the surface electrochemistry and the electrochemically active surface area are not significantly affected by the presence of 30% (v/v) cosolvent. The start of the OER, observed at 1.1 V in 1.0 mol $dm^{-3}$ $HClO_4$, is slightly displaced anodically in the presence of AN, *t*-BuOH and PC. This behaviour is quite distinct for the DMF and DMSO cosolvents for which an intensive current is observed at less anodic potentials (Figure 1). The anticipation of the oxidation current can be attributed to the oxidation of the cosolvent itself, occurring before the OER. This hypothesis is supported by the experimental observation that in the presence of DMSO no gas evolution was observed at the working electrode while in the case of DMF, much less gas evolution takes place when compared to the intense gas evolution observed in the presence of AN, PC and *t*-BuOH cosolvents. These results suggest DMSO oxidation already occurs at much less anodic potentials than the OER. In the case of DMF, the anticipation of the electrolyte discharge current is governed by two events: cosolvent oxidation and OER, cosolvent oxidation prevailing at the lower overpotentials. Direct DMSO and DMF oxidation on Ti/$IrO_2$ was also observed by Zanta et al. [7] in their investigation of the pure solvents. The polarity of the pure solvents being rather similar, these authors considered Gutman's Donor Number, GDN, a parameter which describes the Lewis basicity, to explain the observed behaviour. The GDN values are [12–14]: DMSO (29.8); DMF (26.6); PC (15.1); AN (14.1); $H_2O$ (18.0) and *t*-BuOH (38.0). The higher the basicity of the cosolvent (highest GDN-value) the easier the direct oxidation of the cosolvent. With the exception of *t*-BuOH, the experimentally observed behaviour is consistent with the prediction based on the GDN values. In fact, cosolvents having a GDN higher then water are oxidized before the OER is observed. The GDN-value of 38.0 for *t*-BuOH predicts this solvent should be oxidized rather easily, which is not observed experimentally. A possible explanation for this result is that the hydroxyl group (–OH), localised at a quaternary C, shows a significant shielding effect making the electron transfer more difficult, thus increasing the energy required for its direct oxidation, or be it, the spatial conformation of the ternary alcohol does not favour an appropriate surface orientation.

### 3.2. *Double layer capacity, $C_{dl}$, and rugosity factor*

The double layer capacity, in the presence and absence of 30% (v/v) cosolvent, was determined from the linear relationship [15] obtained between the current (measured at 0.03 V) and the potential sweep rate, *v*, varied between 5 and 100 mV $s^{-1}$ (Figure 2). The $C_{dl}$-values obtained are gathered in Table 1.

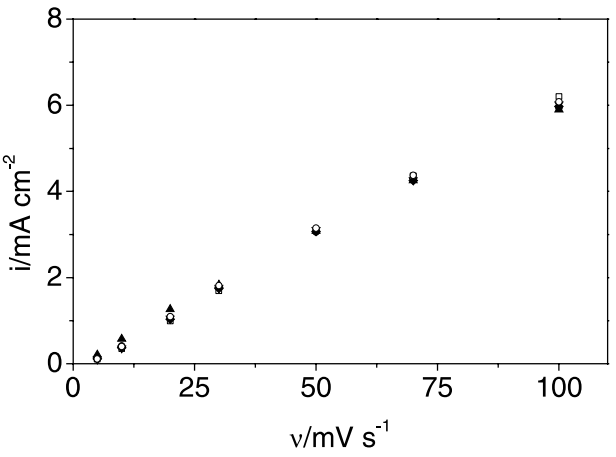


*Fig. 2.* Representative *i* against *v* curves in 1.0 mol $dm^{-3}$ $HClO_4$ in the absence and presence of 30% (v/v) cosolvent. Electrode material: Ti/$Ir_{0.3}Ti_{0.7}O_2$. Key: (□) $H_2O$; (●) AN; (▲) *t*-BuOH; (▽) CP; (◆) DMF; (○) DMSO.

Dividing the experimental $C_{dl}$ results by 0.080 mF $cm^{-2}$, the theoretical value for a planar and smooth $IrO_2$ surface having the rutile structure [16], the rugosity factor, RF, is obtained (Table 1).

Comparison of the data of Table 1 shows that the presence of 30% (v/v) of cosolvent in the supporting electrolyte (1.0 mol $dm^{-3}$ $HClO_4$) or their chemical nature only marginally effect the electrochemically active surface area and the charging process of the electrode coatings. The data also show that the electrochemically active surface area of the binary mixtures is always higher than the pure oxide. This is a frequently observed behaviour attributed to the differences of the physical properties of the individual components in a more complex oxide mixture leading to a higher surface area. The difference in $C_{dl}$/RF-values between both binary oxide mixtures simply reflects the $IrO_2$ content of the coatings.

*Table 1.* Double layer capacity, $C_{dl}$, and roughness factors, *RF*, in the absence and presence of 30% (v/v) cosolvent
Supporting electrolyte: 1.0 mol $dm^{-3}$ $HClO_4$.

| | $C_{dl}$/mF $cm^{-2}$ and *RF** | | | | | |
|---|---|---|---|---|---|---|
| | $H_2O$ | AN | *t*-BuOH | PC | DMF | DMSO |
| Ti/$IrO_2$ | 49 (613) | 46 (575) | 47 (588) | 46 (575) | 44 (550) | 44 (550) |
| Ti/$Ir_{0.7}Ti_{0.3}O_2$ | 71 (888) | 66 (825) | 64 (800) | 70 (875) | 70 (875) | 71 (888) |
| Ti/$Ir_{0.3}Ti_{0.7}O_2$ | 59 (738) | 55 (688) | 53 (663) | 57 (713) | 56 (700) | 56 (700) |

*Values between parenthesis.

### 3.3. *Tafel curves for the oxygen evolution reaction*

#### 3.3.1. *In the absence of cosolvent*

To evaluate the influence of the cosolvent on the OER the electrode kinetics were initially investigated in the absence of cosolvent. Tafel coefficients, after correction for ohmic resistance by the Shub and Reznik procedure [17, 18], and ohmic resistance values are gathered in Table 2.

In the low/high overpotential region, Tafel coefficients of 60/60 mV $dec^{-1}$ and 40/60 mV $dec^{-1}$ were found for the $Ti/IrO_2$ and $Ti/Ir_{0.3}Ti_{0.7}O_2$ nominal coating compositions, respectively. These results are in good agreement with the literature [1]. A 60 mV $dec^{-1}$ Tafel coefficient for the $Ti/IrO_2$ electrode is consistent with the intermediate rearrangement of the oxide surface as the rate-determining step (r.d.s.) [19] ($S–OH^* \rightarrow S–OH$). In the case of the $Ti/Ir_{0.3}Ti_{0.7}O_2$ electrodes the 40/60 mV $dec^{-1}$ values (low/high overpotential regions) are consistent with the electrochemical mechanism ($S–OH \rightarrow S–O + H^+ + e^-$)/intermediate rearrangement ($S–OH^* \rightarrow S–OH$) steps being r.d.s., respectively.

Ohmic resistance values of 0.5–0.6 Ω were found, which are characteristic of this kind of system and are in good agreement with literature data [1].

*Table 2.* Tafel slopes and ohmic resistance in the absence and presence of 30% (v/v) cosolvents

| | | | $b$/mV $decade^{-1}$ | | | | | |
|---|---|---|---|---|---|---|---|---|
| | | | $Ti/IrO_2$ | | | $Ti/Ir_{0.3}Ti_{0.7}O_2$ | | |
| | | | low $\eta$ | high $\eta$ | $R$/Ω | low $\eta$ | high $\eta$ | $R$/Ω |
| $H_2O$ | | 1F* | 60 | 60 | 0.8 | 38 | 62 | 0.6 |
| | | 1B | 60 | 60 | 0.7 | 39 | 62 | 0.5 |
| AN | 1st cycle | 1F | 175 | – | 7.0 | 55 | 68 | 1.3 |
| | | 1B | 341 | – | 3.0 | 67 | 87 | 0.8 |
| | 2nd cycle | 2F† | 176 | – | 7.0 | 57 | 77 | 1.2 |
| | | 2B | 254 | – | 2.0 | 68 | 86 | 0.8 |
| *t*-BuOH | 1st cycle | 1F | 58 | 58 | 1.7 | 43 | 64 | 1.2 |
| | | 1B | 60 | 60 | 1.1 | 48 | 62 | 1.0 |
| | 2nd cycle | 2F | 60 | 60 | 1.7 | 46 | 64 | 1.1 |
| | | 2B | 60 | 60 | 1.1 | 51 | 66 | 1.0 |
| PC | 1st cycle | 1F | | | | 99 | 99 | 2.3 |
| | | 1B | | | | 97 | 97 | 1.8 |
| | 2nd cycle | 2F | | | | 100 | 100 | 1.8 |
| | | 2B | | | | 100 | 100 | 1.7 |
| DMF | 1st cycle | 1F | | | | 169 | 169 | 1.7 |
| | | 1B | | | | 198 | 198 | 0.4 |
| | 2nd cycle | 2F | | | | 184 | 184 | 1.6 |
| | | 2B | | | | 213 | 213 | 0.4 |
| DMSO | 1st cycle | 1F | | | | 99 | 99 | 1.2 |
| | | 1B | | | | 97 | 97 | 1.1 |
| | 2nd cycle | 2F | | | | 100 | 100 | 1.2 |
| | | 2B | | | | 100 | 100 | 1.0 |

*First forward sweep (1F); first backward sweep (1B).
†Second forward sweep (2F); second backward sweep (2B).

#### 3.3.2. *Influence of the cosolvent on the OER*

The influence of the cosolvents on the kinetics and electrode mechanism of the OER was investigated on $Ti/Ir_{0.3}Ti_{0.7}O_2$ recording polarization curves from 1.0 mol $dm^{-3}$ $HClO_4$ supporting electrolyte containing 30% (v/v) cosolvent. In the case of $Ti/IrO_2$, due to the lower stability of this electrode material, the investigation was limited to AN and *t*-BuOH. Representative polarization and Tafel curves are shown in Figures 3 and 4, respectively (Tafel curves are corrected for ohmic drop).

Independent of the cosolvent, a hysteresis effect was observed between consecutive forwards and backwards potential sweeps as well as between the two sets (forwards + backwards) of potential scans (Figure 3). The most intense hysteresis effect was observed with $Ti/IrO_2$ in AN, while hysteresis is much less pronounced in *t*-BuOH or DMSO. This hysteresis effect is explained in terms of surface accommodation/hydration and/or instability of the electrode material.

Kinetic data were obtained from the four Tafel curves (two forwards + two backwards) (Table 2). With the exception of AN at both electrode materials and DMF at $Ti/Ir_{0.3}Ti_{0.7}O_2$, no significant changes in the Tafel coefficients were observed between the forwards and backwards potential sweeps. For both electrode materials and all cosolvents investigated, the experimental Tafel curves present a linear segment, at low overpotentials, followed by a deviation from linearity at the higher overpotentials. After correction for ohmic drop two linear segments were observed for AN and *t*-BuOH at $Ti/Ir_{0.3}Ti_{0.7}O_2$. These results support deviation from linearity, observed in the polarization curves which is due to ohmic drop combined with a change in the r.d.s. of the electrode mechanism. In the case of $Ti/IrO_2$ in *t*-BuOH cosolvent and $Ti/Ir_{0.3}Ti_{0.7}O_2$ in PC, DMF and DMSO cosolvents a single Tafel coefficient was obtained after *iR*-correction, showing deviation from linearity is solely due to ohmic resistance.

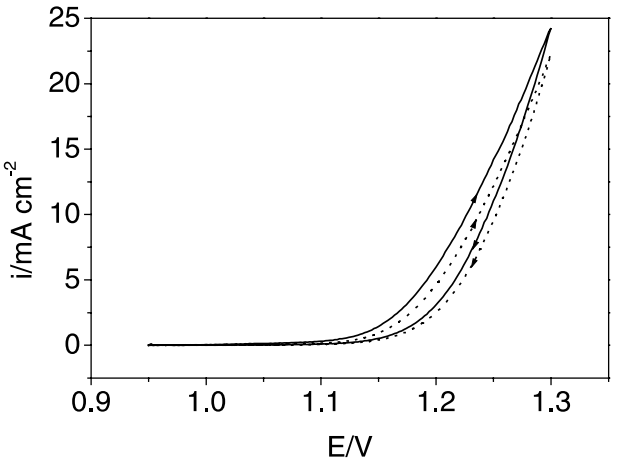


*Fig. 3.* Voltammetric response of an $IrO_2$ electrode, recorded at 0.056 mV $s^{-1}$, in 1.0 mol $dm^{-3}$ $HClO_4$ containing 30% (v/v) *t*-BuOH; first (—) and second (· · · ·) forward and backward potential sweeps; geometric area: 2 $cm^2$.

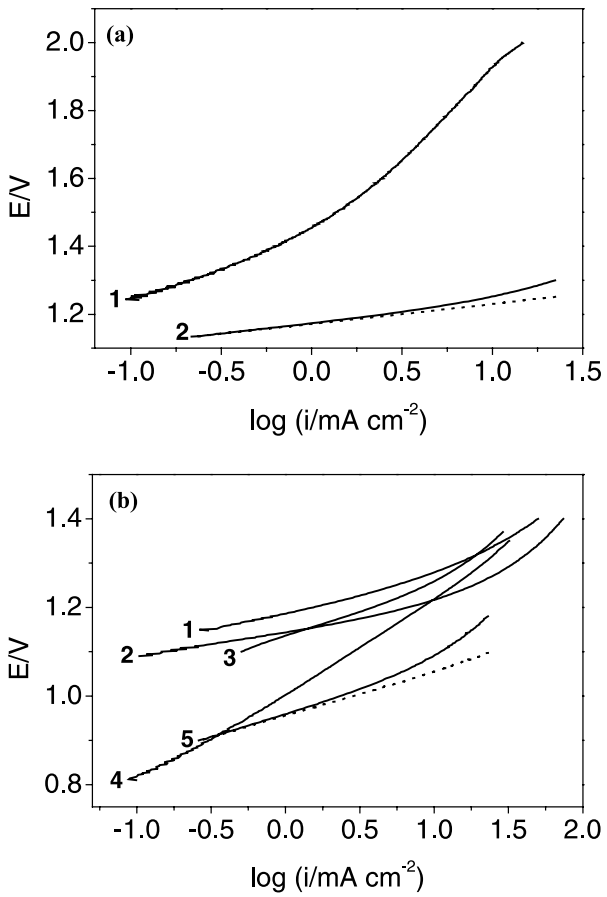


*Fig. 4*. Tafel curves for: (a) $Ti/IrO_2$, (b) $Ti/Ir_{0.3}Ti_{0.7}O_2$. $v = 0.0056$ mV $s^{-1}$. Supporting electrolyte: 1.0 mol $dm^{-3}$ $HClO_4$ containing 30% (v/v) of: (1) AN, (2) *t*-BuOH, (3) PC, (4) DMF, (5) DMSO; (—) experimental curve, (· · · ·) after ohmic drop correction.

It is interesting to observe that *t*-BuOH is the only cosolvent which does not effect the OER electrode kinetics on both electrode materials, contrary to the other cosolvents for which significant changes in the Tafel coefficients are observed. DMSO and DMF also cause a significant anticipation of the anodic current.

To understand the influence of the cosolvent on the voltammetric behaviour and electrode kinetics, features such as changes in the double layer structure, dissolution (corrosion) of the electrode material, intermediate adsorption, oxidation of the cosolvent etc. must be considered. In the absence of an organic cosolvent, the oxide surface is covered with –OH groups (MO(OH)) which are the species participating in the surface solid state redox transitions [1]. In the presence of a significant concentration of organic cosolvent, the formation of species such as MO(S), S representing a cosolvent molecule, is perfectly plausible. This change in the double layer structure makes the approach of a water molecule to the active surface site more difficult. As a result the primary water discharge, which presents a 120 mV Tafel coefficient, becomes the r.d.s. of the OER electrode mechanism. This mechanism satisfactory explains the change in the Tafel coefficient from 60 mV (absence of the cosolvent) to 100 mV in the case of PC. However, this mechanism alone does not explain the *b* values of the other cosolvents, in particularly the value of $b = 100$ mV for DMSO since in this cosolvent a strong anticipation of the voltammetric current is observed together with the absence of gas evolution at the electrode surface.

In the case of DMSO its oxidation by Ir(IV) species is a more plausible explanation for the observed Tafel coefficient of 100 mV. In the case of DMF, the higher Tafel coefficients combined with weak oxygen evolution, suggest that direct DMF oxidation with simultaneous OER are the events governing the electrode process. It is interesting to observe that the Tafel coefficients obtained from the backwards potential scans are systematically, higher then the values obtained from the forwards scans. This result suggests dimerization/polymerization of the radicals, formed during direct DMF oxidation, occurs. The high Tafel coefficients obtained for AN at $Ti/IrO_2$ and DMF at $Ti/Ir_{0.3}Ti_{0.7}O_2$ cannot be explained by the above mentioned mechanisms. According to Krishtalik [20] such high Tafel coefficients find their origin in changes of the surface composition of the electrode material or changes in the electrode process such as active dissolution of the electrode coating. The high Tafel coefficients found in the presence of AN cosolvent suggest active dissolution of the oxide layer combined with the OER are the main electrode process. These electrode process are consistent with the observed gas evolution and the proposal of Martelli et al. [21] who suggest that aliphatic organic cyano compounds are capable of deactivating this kind of electrode material through dissolution of the oxide layer. Experimental evidence to support dissolution of the oxide layer in the presence of AN was obtained by carrying out life tests under condition of accelerated corrosion. $Ti/IrO_2$ and $Ti/Ir_{0.3}Ti_{0.7}O_2$ samples were submitted to a constant anodic current (800 mA $cm^{-2}$) and $E/t$ curves recorded. Service life was taken as the time required for the potential to suddenly change to 6 V. For similar conditions, the literature reports, for aqueous acid conditions, service life data between 560 h [22] ($i = 750$ mA $cm^{-2}$; $T = 70$ °C; 4.0 mol $dm^{-3}$ $H_2SO_4$) and 15 h [23] ($i = 800$ mA $cm^{-2}$; $T = 25$ °C; 1.0 mol $dm^{-3}$ $HClO_4$). In a 1.0 mol $dm^{-3}$ $HClO_4$ containing 30% (v/v) AN supporting electrolyte the $Ti/IrO_2$ electrode showed a service life of 42 h while the $Ti/Ir_{0.3}Ti_{0.7}O_2$ electrode showed a drastically reduced service life of 45 min. For both electrode compositions the Ti-support and the oxide layer were dissolved when the service life was reached. Introduction of $TiO_2$ in an oxide coating is expected to improve the stability of the electrode material [24]. Compared to the pure $Ti/IrO_2$ electrode, the drastic reduction of the service life when the stabilizing oxide is introduced into the $IrO_2$ catalysts suggests $TiO_2$ dissolution takes place causing electrode deactivation.

Besides active dissolution of the oxide layer with simultaneous OER direct AN oxidation, resulting in a resistive film partially blocking the electrode surface, cannot be descarded to explain the high Tafel

coefficients. Such a film can be easily formed through dimerization/polymerization of the intermediates of AN oxidation. Experimental evidence to support this proposal is found in the much higher ohmic resistance values found for $Ti/IrO_2$ in the presence of AN cosolvent.

It is interesting to observe that substitution of 70% mol $IrO_2$ by $TiO_2$ (see Table 2) brings both the Tafel coefficients and the ohmic resistance to "normal" values within the general picture of the several cosolvents investigated. The ohmic resistance values found (Table 2) are compatible with metallic conductive oxide coatings submerged in a supporting electrolyte having good conductivity. Electrochemical impedance spectroscopic investigations of similar systems in 1.0 mol $dm^{-3}$ $HClO_4$ [25] has shown that the main contribution to the ohmic resistance comes form the solution resistance. The data gathered in Table 2 reveal a small increase of the ohmic resistance when a cosolvent is introduced to the 1.0 mol $dm^{-3}$ $HClO_4$ supporting electrolyte, which is consistent with the decrease in conductivity of mixed solvents. As discussed above, an exception to this behaviour is $Ti/IrO_2$ in the presence of the AN as cosolvent.

### 3.4. *Electrode stability*

The stability of the electrode materials was monitored using the anodic voltammetric charge, $Q_a$, obtained by integration of the anodic branch of the CV, recorded covering the 0.2–1.0 potential interval from an aqueous 1.0 mol $dm^{-3}$ $HClO_4$, without cosolvent. Results at selected moments during the investigation are gathered in Table 3.

Consistent with other results [26] both electrode materials show excellent stability in the absence of cosolvent, even under conditions of intense oxygen evolution. With the exception of AN, all cosolvents reveal the same general behaviour showing the electrochemically active surface area or the stability of the electrode materials is not affected by the cosolvent.

The significant decrease of $Q_a$ observed after the Tafel curve investigation in the presence of AN cosolvent (~37% for $Ti/IrO_2$; ~18% for the $TiO_2$ stabilized $IrO_2$ coating) could, in principle, be due to partial blocking of the solid state surface redox transitions. Since the SSSRT process only involves $H^+$ injection/ejection and $H^+$ is a small species it is reasonable to assume the $H^+$ injection/ejection process is not significantly affected. This assumption is supported by the $Q_a$ results of the other aprotic cosolvents investigated, for which no significant changes were observed. So the main event explaining the significant decrease of $Q_a$ must be coating dissolution (especially the $TiO_2$ component) by AN as supported by the service life data. The lower $Q_a$ decrease observed for the $Ti/Ir_{0.3}Ti_{0.7}O_2$ electrode is in 'apparent' contradiction with the service life data. However, the later results were obtained under drastically different experimental conditions (much higher anodic current). The much higher electrochemically active surface area of the binary mixture (Table 3) also results in a lower effective current density when compared to the $Ti/IrO_2$ coating.

*Table 3.* Anodic voltammetric charge, $Q_a$, obtained by integration of the 0.2–1.0 potential interval

| | $Q_a$/mC | | | | | |
|---|---|---|---|---|---|---|
| | $Ti/IrO_2$ | | | $Ti/Ir_{0.3}Ti_{0.7}O_2$ | | |
| | Before | 1st Tafel | 2nd Tafel | Before | 1st Tafel | 2nd Tafel |
| $H_2O$ | 70 | 66 | 66 | 281 | 298 | 293 |
| $CH_3CN$ | 51 | 32 | 32 | 299 | 263 | 243 |
| *t*-BuOH | 65 | 62 | 61 | 251 | 251 | 247 |
| CP | – | – | – | 300 | 298 | 298 |
| DMF | – | – | – | 228 | 230 | 229 |
| DMSO | – | – | – | 340 | 343 | 345 |

## 4. Conclusions

The presence of 30% (v/v) cosolvent in 1.0 mol $dm^{-3}$ $HClO_4$ or the chemical nature of the cosolvent do not displace the SSSRT nor significantly affect the electrochemically active surface area of $IrO_2$-based oxide electrodes. The OER is slightly displaced anodically in the presence of *t*-BuOH, AN and PC while DMF and DMSO cause a significant anticipation of the voltammetric current, attributable to the oxidation of these cosolvents. *t*-BuOH is the only cosolvent which does not affect the OER electrode kinetics. Tafel coefficients obtained in the presence of PC suggest a change in the r.d.s. of the OER electrode mechanism, while in the case of DMF, DMSO and AN, besides affecting the OER electrode mechanism, other complications, such as coating dissolution (AN) or cosolvent oxidation (DMSO, DMF), were evident. Electrode stability is excellent in the presence of 30% (v/v) *t*-BuOH, PC, DMSO and DMF, in contrast to AN, for which strong electrode dissolution was observed, as supported by voltammetric charge and service life data. The use of a stabilizing oxide ($TiO_2$) reduces (current not exceeding ~100 mA), but does not avoid, electrode deactivation. Thus, AN cannot be recommended as a cosolvent. Ohmic resistance of the systems increases only slightly in the mixed solvents and is consistent with the changes in conductivity caused by the partial substitution of water by the cosolvent.

## Acknowledgements

The authors acknowledge financial support from the CNPq and FAPEMIG Foundations.

## References

1. S. Trasatti (Ed.), 'Electrodes of Conductive Metallic Oxides', Parts A and B (Elsevier Science, Amsterdam, 1980/1981).

2. J. Krýsa, J. Maixner, R. Mráz and I. Rousar, *J. Appl. Electrochem.* **28** (1998) 369.
3. J. Krýsa, L. Kule, R. Mráz and I. Rousar, *J. Appl. Electrochem.* **26** (1996) 999.
4. Ch. Comninellis and A. De Battisti, *J. Chim. Phys.* **93** (1996) 673.
5. G. Fóti, D. Gandini and Ch. Comninellis, *Curr. Top. in Eletrochem.* **5** (1997) 71.
6. A.M. Couper, F.C. Walsh and D. Pletcher, *Chem. Rev.* **90** (1990) 837.
7. C.L.P.S. Zanta, A.R. de Andrade and J.F.C. Boodts, *Electrochim. Acta* **44** (1999) 3333.
8. A.R. de Andrade, J.F.C. Boodts and C.L.P.S. Zanta, Abstract 964, p. 1206, The Electrochemical Society Meeting Abstracts, Vol. 96-1, Los Angeles, CA, 5–10, May (1996).
9. P.G. Pickup and V.I. Birss, *J. Electrochem. Soc.* **135** (1988) 41.
10. L.A. Silva, V.A. Alves, M.P.A. Silva, S. Trasatti and J.F.C. Boodts, *Electrochim. Acta.* **42** (1997) 271.
11. E.J.M. O'Sullivan and J.R. White, *J. Electrochem. Soc.* **136** (1989) 2576.
12. D.T. Sawyer and J.L. Roberts, Jr, 'Experimental Electrochemistry for Chemists' (J. Wiley & Sons, 1974), p. 174.
13. Y. Marcus, *Chem. Soc. Rev.* (1993) 409.
14. M. Sandström, I. Person and P. Person, *Acta Chem. Scand.* **44** (1990) 653.
15. R.N. Singh, J.F. Köenig, G. Poillerat and P. Chartier, *J. Electrochem. Soc.* **137** (1990) 1408.
16. P. Siviglia, A. Daghetti and S. Trasatti, *Colloids Surf.* **7** (1983) 15.
17. D.M. Shub and M.F. Reznik, *Elektrokhimiya* **21** (1985) 855.
18. D.M. Shub, M.F. Reznik and V.V Shalaginov, *Elektrokhimiya* **21** (1985) 937.
19. S. Trasatti, *in* H. Wendt (Ed.), 'Electrochemical Hydrogen Technologies' (Elsevier Science, Amsterdam, 1990).
20. L.I. Krishtalik, *Electrochim. Acta* **26** (1981) 329.
21. G.N. Martelli, R. Ornelas and G. Faita, *Electrochim. Acta* **39** (1994) 1551.
22. S.M. Lin and T-C. Wen, *J. Electrochem. Soc.* **140** (1993) 2265.
23. T.A.F. Lassali, J.F.C. Boodts and L.S. Bulhões, *J. Appl. Electrochem.* **30** (2000) 625.
24. V.V. Gorodetskii, V.A. Neburchilov and M.M. Pecherskii, *Russ. J. Electrochem. (Transl. Elektrokhimiya)* **30** (1994) 916.
25. T.A.F. Lassali, J.F.C. Boodts and L.O.S. Bulhões, *Electrochim. Acta.* **44** (1999) 4203.
26. L.A. Silva, V.A. Alves, M.P.A. Silva, S. Trasatti and J.F.C. Boodts, *Can. J. Chem.* **75** (1997) 1483.